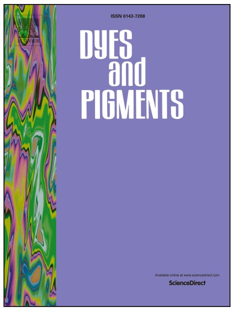

Phenothiazine-oxadiazole push-pull fluorophores: Combining high quantum efficiency, excellent electrochemical stability and facile functionalization

Michael Y. Wong, Louis M. Leung

PII: S0143-7208(17)30818-5
DOI: 10.1016/j.dyepig.2017.06.054
Reference: DYPI 6075

To appear in: *Dyes and Pigments*

Received Date: 12 April 2017
Revised Date: 15 June 2017
Accepted Date: 21 June 2017

Please cite this article as: Wong MY, Leung LM, Phenothiazine-oxadiazole push-pull fluorophores: Combining high quantum efficiency, excellent electrochemical stability and facile functionalization, *Dyes and Pigments* (2017), doi: 10.1016/j.dyepig.2017.06.054.

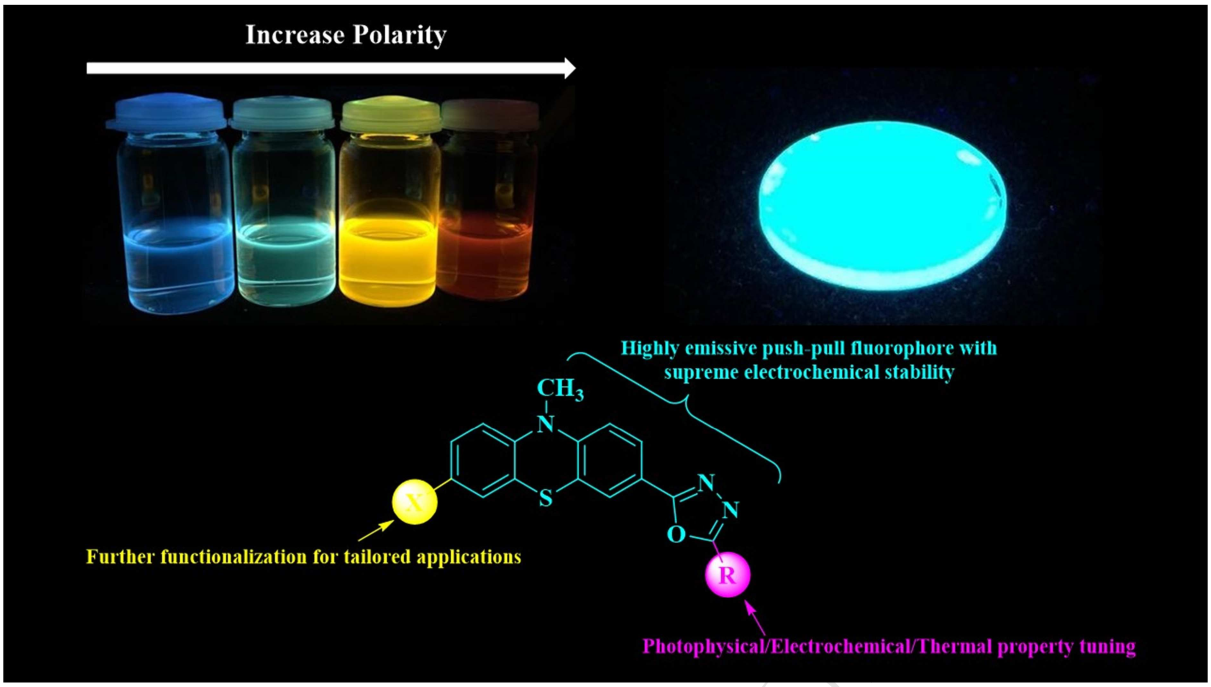
Increase Polarity
Highly emissive push-pull fluorophore with supreme electrochemical stability
CH3
N
S
N
N
O
X
R
Further functionalization for tailored applications
Photophysical/Electrochemical/Thermal property tuning

Phenothiazine-Oxadiazole Push-Pull Fluorophores: Combining High Quantum Efficiency, Excellent Electrochemical Stability and Facile Functionalization

Michael Y. Wong*[a] and Louis M. Leung[a]

[a]*Department of Chemistry, Hong Kong Baptist University, Kowloon Tong, Hong Kong SAR, China. E-mail: myw1011@gmail.com*

Abstract

A series of five novel sky-blue to green emitting push-pull fluorophores based on phenothiazine donor and 1,3,4-oxadiazole acceptor were synthesized and characterized. Their doped thin films (5 wt% in PMMA) showed high quantum efficiencies (Φ_{PL}) from 0.63 to 0.77. These fluorophores also underwent remarkably reversible oxidations and reductions suggesting their excellent electrochemical stability. Facile tuning of photophysical, thermal and electrochemical properties of the fluorophores could be achieved by optimizing the functional group attached to the 1,3,4-oxadiazole moiety. Finally, we propose that further functionalization of these fluorophores can be easily achieved and as a proof of concept the synthesis of a vinyl polymer derivative **Poly(PO-Tol)** was demonstrated.

(Keywords: push-pull; donor-acceptor; structure-property relationship; intramolecular charge-transfer)

Introduction

Push-pull donor-acceptor (D-A) architecture has been extensively employed in optoelectronic materials [1-13]. For example, thermally activated delayed fluorescence (TADF) is a recent important advance in organic light-emitting diode (OLED) technology for singlet harvesting without the use of organometallic complexes based on rare metals, the gist of which requires a D-A architecture to separate the highest occupied molecular orbital (HOMO) and lowest unoccupied molecular orbital (LUMO) so that a vanishing splitting energy (ΔE_{ST}) is realized [1-6]. In addition, D-A architecture is essential in many organic photovoltaics (OPV) materials to facilitate charge dissociation and to extend their absorption into the visible region [7-11].

Phenothiazine is a favorable constituent in many optoelectronic materials due to its numerous attractive intrinsic properties. Firstly, termed elegantly as “butterfly conformation”, the two phenyl rings of phenothiazine are twisted, so that undesirable intermolecular interactions such as excimer formation can be suppressed [7-8,14-15]. This structural feature is essential for dye-sensitized solar cells (DSSCs) because aggregation of phenothiazine-based dyes is suppressed so that higher power conversion efficiencies can be achieved [7-8]. Secondly, phenothiazine also forms highly stable radical cation with outstanding electrochemical stability [16-17]. Finally, facile transformation of phenothiazine to *S*,*S*-dioxide analogues enables convenient photophysical, thermal and electrochemical properties engineering which can bring improved performances in electroluminescence efficiency [18-21]. On the other hand, 1,3,4-oxadiazole is a very popular *n*-type material due to its excellent electron-injection and electron-transporting capabilities and has been utilized in chemosensors [22-23], organic semiconductors [24-26] and electroluminescence devices [5,27-28].

Nevertheless, phenothiazine-oxadiazole D-A small molecules with intramolecular charge-transfer (ICT) character have been underexplored. The work contributed by Park and co-workers contained a small molecule where phenothiazine was linked to

1,3,4-oxadiazole via a phenyl bridge but it was a synthetic intermediate whose physical properties were not studied [29]. Pan *et al*. reported 10-ethyl-3-(5-methyl-1,3,4-oxa-diazol-2-yl)-10*H*-phenothiazine which was structurally very similar to compound **5** in this study (*vide infra*), but only the crystal structure was studied [30]. In a patent filed by Ahn *et al*., two phenothiazine-oxadiazole push-pull fluorophores were applied as emitters in OLED devices [31]. In addition, Qiu *et al.* very recently employed two phenothiazine-oxadiazole fluorophores in the emitting layer of OLED devices and achieved a maximum external quantum efficiency (EQE) of 5.4% which is close to the theoretical EQE cap for fluorescent OLEDs, clearly demonstrating the potency of this class of emitters [5]. However, the phenothiazine-oxadiazole push-pull fluorophores reported by Ahn and Qiu were structurally very similar and therefore it leaves room for further investigation of this emitter system. In this contribution, we synthesized and characterized a series of five novel phenothiazine-oxadiazole D-A fluorophores (Figures **1**, **5-9**) where the substituents attached to the oxadiazole moiety were responsible for tuning the photophysical, electrochemical and thermal properties of the fluorophores. A *S,S*-dioxide analogue **PO-Tol-SO2** (**10**) (Figure **1**, inset) was also synthesized where the oxidized phenothiazine resulted in tremendous impact on the photophysical and electrochemical profiles of these fluorophores due to the loss of their push-pull character [18]. We shall demonstrate that the phenothiazine-oxadiazole D-A fluorophores are not only highly emissive but also electrochemically very stable. Finally, facile functionalization of these D-A fluorophores for tailored purposes is another attractive merit of this emitter system and we shall demonstrate this by preparing a vinyl polymer derivative **Poly(PO-Tol)**.

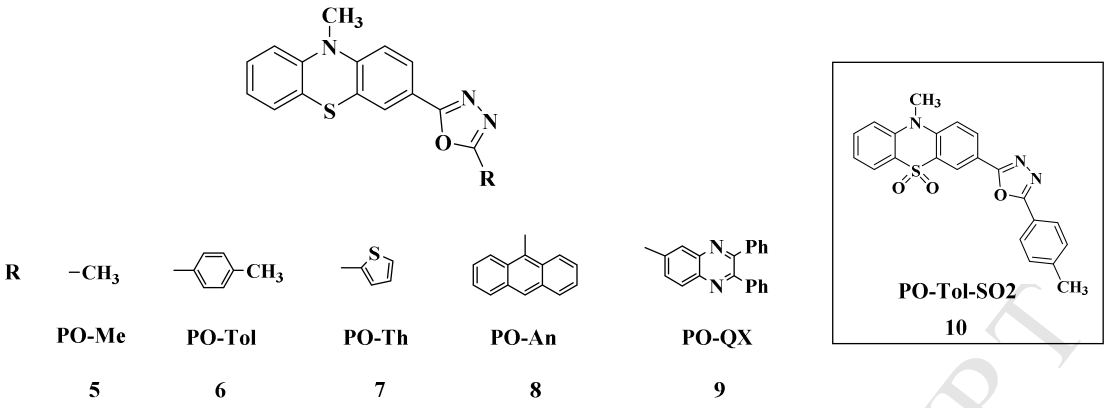

Figure **1**. Chemical structures of the novel phenothiazine-oxadiazole D-A fluorophores (**5-9**). Also shown in the inset is **PO-Tol-SO2** (**10**) which is the *S,S*-dioxide analogue of **PO-Tol (6)**.

Results and Discussions

Synthesis

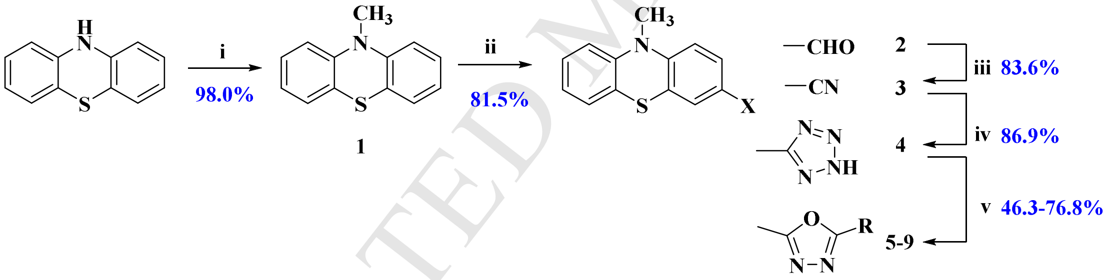

Scheme **1**. Synthesis of phenothiazine-oxadiazole D-A fluorophores. i) K^+*t*-BuO^-, MeI, THF, rt, 30 min ii) $POCl_3$, DMF, chlorobenzene, 70 ^oC, 5 h iii) $NH_2OH·HCl$, NMP, 120 ^oC, overnight iv) NaN_3, NH_4Cl, DMF, 115 ^oC, 2 d v) RCOCl, pyridine, reflux, overnight.

The synthetic route of the phenothiazine-oxadiazole D-A fluorophores **5-9** is shown in Scheme **1**. The key intermediate tetrazole **4** was generated by Vilsmeier formylation, cyanation and subsequent cyclization by azide anion. The target 1,3,4-oxadiazole was formed by reacting **4** with corresponding acid chlorides in refluxing pyridine. The *S,S*-

dioxide analogue **PO-Tol-SO2** (**10**) was derived from **PO-Tol** (**6**) in an excellent yield of 99.3% using *m*-chloroperoxybenzoic acid (mCBPA) as the oxidant. All the syntheses employed conventional chemistry and can be easily scaled up.

Photophysical Properties

Table **1**. Summary of absorption and emission profiles of the phenothiazine-oxadiazole D-A fluorophores in different matrices.

	Absorption	Emission[a]				
	λ_{abs} (nm) [ε] (10^3 M^{-1} cm^{-1})	λ_{em} (nm) [FWHM[b]] (nm)				
	DCM	PhMe	DCM	ACN	Film[c]	Φ_{sol}/Φ_{film}[d]
5	269 [34.1], 277 [32.2], 348 [6.9]	464 [67]	482 [72]	493 [77]	465 [72.5]	0.51/0.72
6	290 [32.3], 364 [11.5]	477 [68.5]	494 [72.5]	502 [80.5]	484 [70]	0.65/0.77
7	298 [27.8], 368 [13.8]	482 [68]	499 [75.5]	510 [88.5]	484 [68]	0.64/0.73
8	280 [27.0], 364 (sh) [12.7], 387 [13.8]	488 [94]	529 [106]	627 [144.5]	498 [104]	0.51/0.69
9	275 [35.0], 302 (sh) [26.4], 387 [18.6]	530 [94.5]	664 [138.5]	–[d]	529 [110.5]	0.51/0.63
10	261 [16.8], 273 [18.2], 291 [23.8], 332 [43.2]	375 [44]	375 [45]	380 [51.5]	378 [42]	0.50/0.55

[a] λ_{ex} = 360 nm. [b]Full width at half-maximum. [c]Spun-coated thin film with 5 wt% sample in PMMA. [d]Solution PLQY (Φ_{sol}) was measured in toluene with quinine sulfate as the reference (PLQY = 0.55 in 1*N* H_2SO_4 at 298 K). [d]Emission too weak to be detectable.

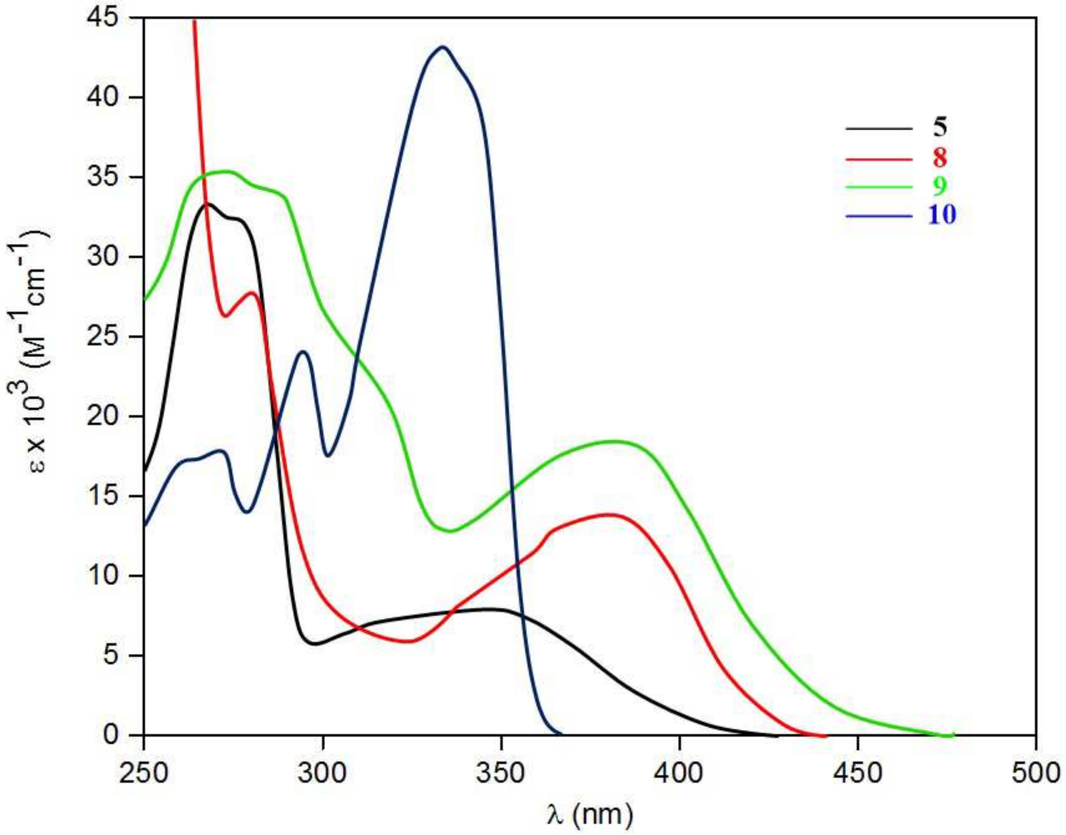

Figure **2**. Absorption spectra of the phenothiazine-oxadiazole D-A fluorophores (**5**, **8** and **9**) and the *S,S*-dioxide analogue (**10**) in DCM.

Table **2** summarizes the photophysical properties of the phenothiazine-oxadiazole D-A fluorophores and Figure **2** shows the absorption spectra of some phenothiazine-oxadiazole D-A fluorophores under optically dilute solutions in DCM. All the D-A fluorophores (**5-9**) exhibited both π-π* transitions from ~280 nm to ~300 nm and intramolecular charge transfer (ICT) bands from ~350 nm to ~390 nm [32-34]. However, the ICT band was absent in **10** due to the loss of electron-donating ability of the phenothiazine moiety after the introduction of *S,S*-dioxide functional group [18]. In general, the ICT absorption maxima depended on the conjugation lengths and the electronic effects of the functional group attached to the oxadiazole moiety. For example, **5** showed the highest-energy ICT absorption maximum at 348 nm due to shortest conjugation length of the methyl group. Replacements of methyl group with toluyl and thiophene functionalities increased conjugation lengths and resulted in red-shifts in ICT band by 16 nm and 20 nm as observed in **6** and **7** respectively. On the other hand, **9** showed the lowest-energy ICT absorption maximum at 387 nm due to the electron-withdrawing 2,3-diphenylquinoxaline group. The absorption maxima of the D-A fluorophores were nearly identical irrespective of the solvents (Supporting Information Table **S1**), suggesting the absence of positive solvatochromism due to their relatively low polarity in the ground state [35-39].

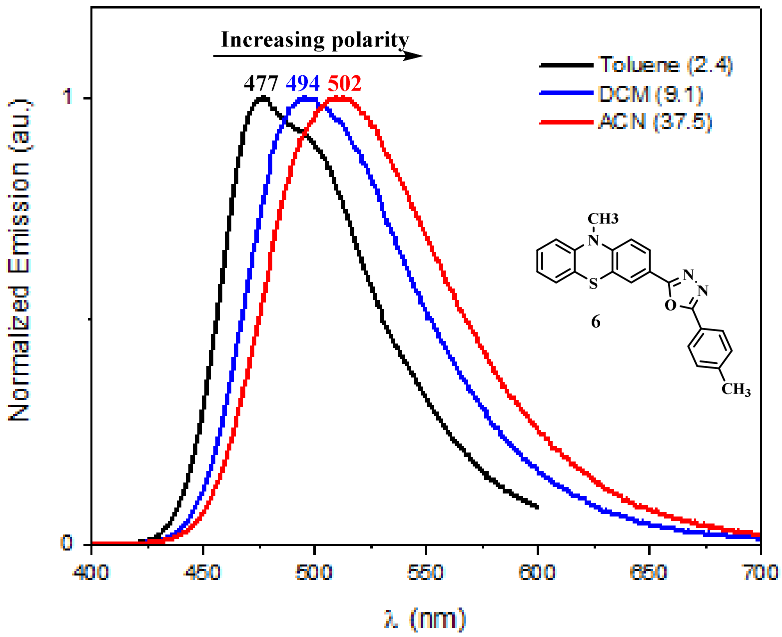

Figure **3**. Normalized emission spectra of **6** in toluene, DCM and acetonitrile (solvent dielectric constants ε listed in bracket) [40] showing positive solvatochromism.

The phenothiazine-oxadiazole D-A fluorophores thin films (5 wt% in PMMA) exhibited high quantum efficiencies (0.63-0.77) and in particular **5-7** emitted sky-blue light (λ_{PL}: 465-484 nm), suggesting their high potential as emitters for OLED applications. In general, the quantum efficiencies in toluene (0.51-0.64) were lower than those of thin films which can be explained by the more rigid matrix in the latter to suppress non-radiative quenching pathways [4]. The emission energies of the phenothiazine-oxadiazole D-A fluorophores demonstrated a similar trend as the absorption profile and could be easily tuned by the functional group attached to the oxadiazole moiety. For example, while **5** showed the bluest emission (film λ_{PL}: 465 nm), **9** gave the lowest emission energy (film λ_{PL}: 529 nm) among the series with the help of strongly electron-withdrawing 2,3-diphenylquinoxaline group. However, unlike the absorption study which showed little dependence on the choice of solvents, positive solvatochromism was evident in the emission spectra. For example, the emission maxima of **6** red-shifted when the polarity of the solvents increased (Figure **3**) which was due to the dipolar stabilization of the highly polar excited state [35-39]. When the phenothiazine was oxidized to *S,S*-dioxide, the D-A architecture was lost and hence no positive solvatochromism was observed in **10** [18].

Electrochemical Properties

Table **2**. Summary of electrochemical profiles of the phenothiazine-oxadiazole D-A fluorophores by cyclic voltammetry.[a]

	Oxidations			Reductions			
	$E_{1/2}^{ox}$ (V vs Fc/Fc$^+$)	$\Delta E_p^{ox\,b}$ (mV)	HOMO^c (eV)	$E_{1/2}^{red}$ (V vs Fc/Fc$^+$)	$\Delta E_p^{red\,d}$ (mV)	LUMO^e (eV)	Band gap (eV)
5	0.44	73	-5.24	-2.57	71	-2.23	3.01
6	0.44	79	-5.24	-2.51	64	-2.29	2.95
7	0.44	68	-5.24	-2.49	76	-2.31	2.93
8	0.46	75	-5.26	-2.38	74	-2.42	2.84
9	0.46	76	-5.26	-2.28	73	-2.52	2.74
10	1.39	–^{f}	-6.19	-2.05	74	-2.75	3.44

[a] Measured in degassed THF under argon with 0.1 M nBu$_4$NPF$_6$ as the supporting electrolyte. [b] Peak-to-peak separations for oxidation processes. [c] HOMO energies were calculated using the

---

relation $E_{HOMO} = -(E_{1/2}^{ox} + 4.8)$ eV, where $E_{1/2}^{ox}$ is the oxidation potential with respect to $E_{1/2}$ of ferrocene/ferrocenium redox couple. [d]Peak-to-peak separations for reduction processes. [e]LUMO energies were calculated using the relation $E_{LUMO} = -(E_{1/2}^{red} + 4.8)$ eV, where $E_{1/2}^{red}$ is the reduction potential with respect to $E_{1/2}$ of ferrocene/ferrocenium redox couple. [f]Irreversible oxidation.

The electrochemical properties of the phenothiazine-oxadiazole D-A fluorophores were studied by cyclic voltammetry in degassed THF under argon with 0.1 M $n\mathrm{Bu_4NPF_6}$ as the supporting electrolyte and the data are summarized in Table **2**. Fluorophores **5-9** possessed similar HOMO energy levels (from -5.24 eV to -5.26 eV) which suggested that the HOMO was mainly located on the phenothiazine moiety and the functional groups attached on the oxadiazole moiety were too remote to have observable effect on the HOMO. On the contrary, the LUMO energy levels were strongly affected by the substituents attached on the oxadiazole. For example, 9-anthracenyl and 6-(2,3-diphenylquinoxalinyl) groups resulted in much deeper LUMO energy levels of -2.42 eV and -2.52 eV respectively in **8** and **9**, suggesting the LUMOs were subjected to conjugation length and electron-withdrawing effects of the substituents. These fluorophores also showed highly reversible oxidations and reductions due to remarkably stable phenothiazine radical cation and oxadiazole radical anion, as demonstrated in Figure **4** that the cyclic voltammogram profile of **6** did not change at all after 10 repeated cycles. Hence, the fluorophores have excellent redox reversibility which is crucial to the stability of optoelectronic devices. In addition, the peak-to-peak separations for both oxidations (ΔE_p^{ox}) and reductions (ΔE_p^{red}) of fluorophores **5-9** ranged from 68 to 79 mV and from 64 to 79 mV respectively, which are close to the theoretical 59 mV for an one-electron process. Oxidation of the phenothiazine strongly suppressed the donor ability of the phenothiazine moiety and the HOMO was sharply lowered by as large as ~1 eV (compare **6** and **10**). The oxidation of **10** also became irreversible.

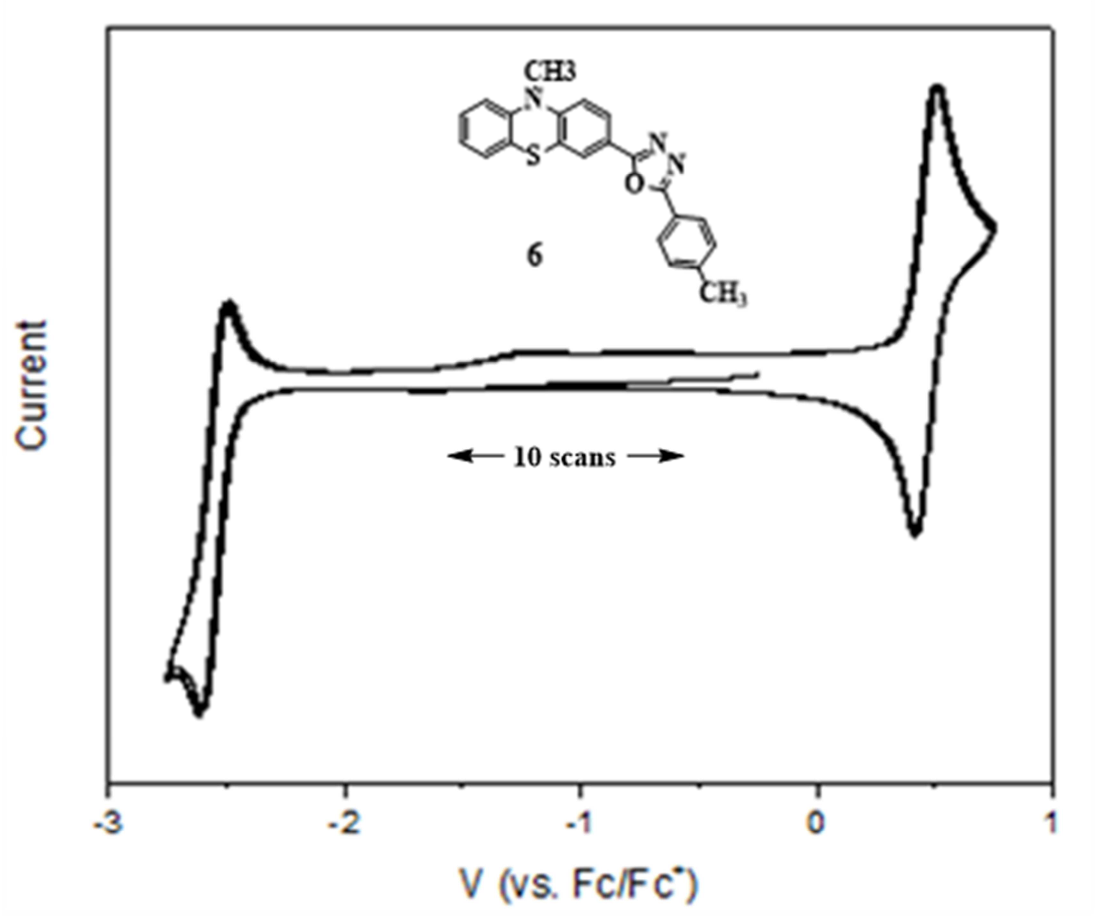

Figure **4**. Cyclic voltammogram of **6** in degassed THF with 0.1 M *n*Bu$_4$NPF$_6$ as the supporting electrolyte for 10 cycles. Both the oxidation and reduction were highly reversible and did not change at all after 10 repeated scans, suggesting desirable electrochemical stability of this class of phenothiazine-oxadiazole D-A fluorophores.

Thermal Properties

Table **3**. Summary of thermal properties of the phenothiazine-oxadiazole D-A fluorophores.

	T_g[a] (°C)	T_m[b] (°C)	T_{onset}[c] (°C)
5	–[d]	170	365

6	–[d]	144	408
7	103	168	408
8	104	235	419
9	125	245	446
10	104	252	474

[a]Glass-transition temperature. [b]Melting point [c]Decomposition onset temperature at 5 wt% loss. [d]Not detected.

The glass-transition temperatures (T_g) and the decomposition onset temperatures (T_{onset}) of the phenothiazine-oxadiazole D-A fluorophores were probed by differential scanning calorimetry (DSC) and thermogravimetric analysis (TGA) techniques respectively and the results are summarized in Table **3**. DSC and TGA thermograms of some D-A fluorophores are shown in Supporting Information (Figure **S17**-**S19**). High T_g is crucial to the film morphological stability against crystallization due to joule heat formation during the OLED device operation [41-42]. It is evident that the choice of functional group attached to the oxadiazole moiety could affect the T_g of the D-A fluorophores. For example, the incorporation of 2,3-diphenylquinoxaline group in **9** greatly enhances T_g to 125^{o}C due to its higher molecular weight [43-44] and polarity [43,45]. In addition, oxidation of the phenothiazine to *S,S*-dioxide results in higher thermal stability which can be deduced by comparing the T_g, melting point and onset decomposition temperature (T_{onset}) between fluorophores **10** and **6**. In general, the phenothiazine-oxadiazole D-A fluorophores are thermally robust with $T_g > 100^{o}$C and $T_{onset} > 400^{o}$C which suit optoelectronic applications.

Further functionalization of phenothiazine-oxadiazole D-A fluorophores for additional property

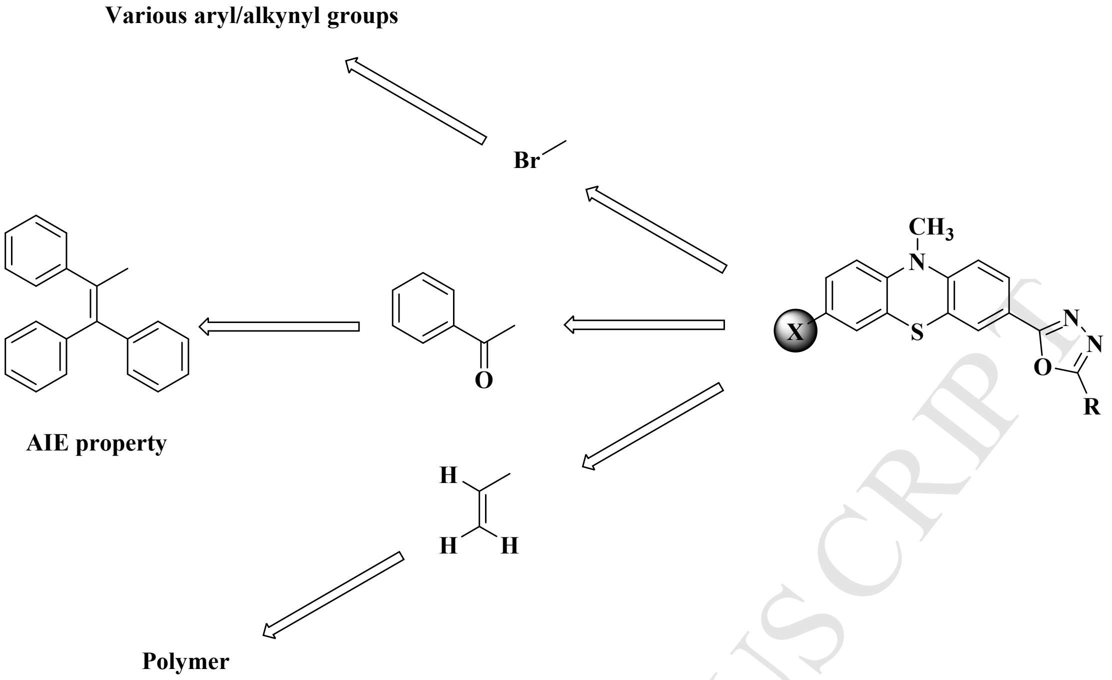

Scheme **2**. A map showing a number of possible further functionalizations of the phenothiazine-oxadiazole D-A fluorophores for tailored applications. Bromination followed by Suzuki or Sonogashira coupling gives a variety of aryl and alkynyl groups respectively (top route). Friedel-Crafts acylation followed by Knoevenagel condensation offers the tetraphenylethylene group for AIE property (middle route). Vilsmeier formylation followed by Wittig reaction gives vinyl monomer which can be readily polymerized, which was actually achieved in this study (bottom route).

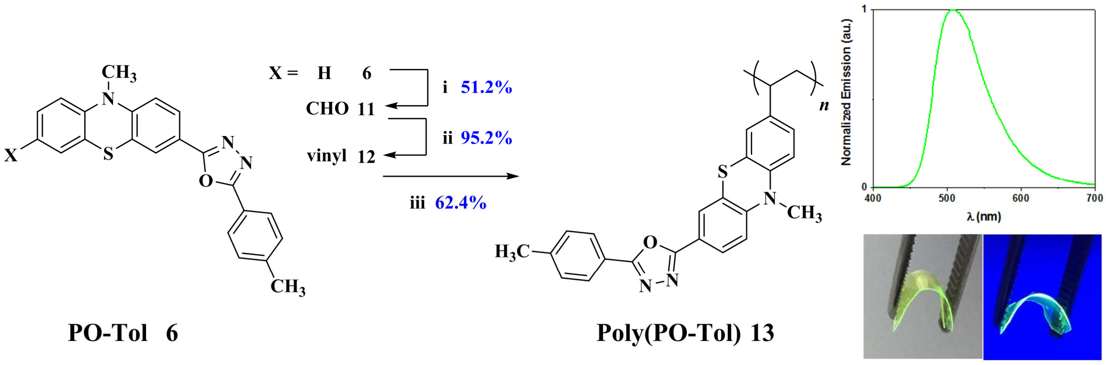

Scheme **3**. Preparation of vinyl polymer **Poly(PO-Tol)** (**13**) derived from **PO-Tol** (**6**). i) $POCl_3$, DMF, chlorobenzene, 100 °C, overnight ii) K^+*t*-BuO^-, $CH_3Ph_3P^+Br^-$, THF, rt, 30 min. iii) AIBN, toluene, 80°C, overnight. Shown at the right are the normalized emission of the polymer neat film and its photos of being held by a forceps demonstrating excellent flexibility in ambient condition (left) and under ultra-violet irradiation (right).

An additional merit of the phenothiazine-oxadiazole D-A fluorophores is facile functionalization at the other side of the phenothiazine moiety (i.e. 7-position), thanks to its strong *p*-type character and highly regioselective electrophilic aromatic substitution reactions. As shown in Scheme **2**, the phenothiazine-oxadiazole D-A fluorophores can be brominated followed by Suzuki or Sonogashira coupling to generate desired aryl or alkynyl derivatives. The fluorophores can also carry out Friedel-Crafts acylation with benzoyl chloride followed by Knoevenagel condensation with diphenylmethane to yield the tetraphenylethylene functionality which should bring about the interesting aggregation-induce emission (AIE) property [46]. As a proof of concept, we synthesized a vinyl polymer **Poly(PO-Tol)** (**13**) based on **PO-Tol** (**6**) as shown in Scheme **3**. The D-A fluorophore **PO-Tol** (**6**) underwent Vilsmeier formylation at position 6 to give **11** in a 51.2% yield, followed by Wittig reaction with methyl triphenylphosphonium bromide as the ylide precursor to generate the vinyl monomer **12** with an excellent yield of 95.2%. Conventional free-radical polymerization using catalytic AIBN initiator (1 mol%) in toluene at 80^{o}C offered **Poly(PO-Tol)** in a 62.4% yield with a high number-average molecular weight (M_n) of 32,000 Da and a polydispersity index (PDI) of 1.7. The neat film of **Poly(PO-Tol)** showed a green emission (λ_{PL}: 507 nm) with a high quantum efficiency of 67%. Therefore, the polymer is an ideal candidate as the emitting layer in organic light-emitting diodes (OLED) or in light-emitting electrochemical cells (LECs) for its highly reversible oxidation and reduction (*vide supra*) which is beneficial to LEC device performance [47].

Conclusions

In this study, we have synthesized and characterized a series of five novel phenothiazine-oxadiazole push-pull fluorophores whose photophysical, electrochemical and thermal properties could be conveniently tuned by the oxadiazole substituents. These fluorophores were found to be highly emissive and electrochemically stable. We have also demonstrated their facile functionalization by preparing a vinyl polymer derivative. Therefore, we believe that this class of phenothiazine-oxadiazole push-pull fluorophores are very promising materials in optoelectronic applications.

Experimental Section

Characterization. Analytical thin-layer-chromatography (TLC) was performed with silica plates with aluminum backings (250 µm with F-254 indicator). TLC visualization was accomplished by 254/365 nm UV lamp. ^{1}H and ^{13}C NMR spectra were recorded with a Bruker-AF301 AT 400 MHz spectrometer using $CDCl_3$ as solvent and tetramethylsilane as the internal standard. High resolution mass spectrometry (HRMS) was carried out using a Bruker autoflex MALDI-TOF mass spectrometer. Elemental analyses were performed using a Perkin-Elmer 2400 Series II Analyzer. Melting points were taken on differential scanning calorimetry (DSC) or on a MEL-TEMP capillary tube apparatus without correction. UV-vis absorption spectra were measured in THF at a 100 ppm concentration using a Varian Cary 200 spectrophotometer. Fluorescence spectra were measured in toluene/DCM/MeCN at a 10 ppm concentration using a Perkin Elmer LS55 Luminescence Spectrometer. Quantum yields were measured in toluene with quinine sulfate in 1*N* sulfuric acid as the standard (Φ=0.55) with reference to the equation $\Phi_s = \Phi_r(A_r/A_s)((I_s/I_r)(n_s/n_r)^2$, where A stands for the absorbance at the excitation wavelength (λ_{ex}: 360 nm), I is the integrated area under the corrected emission curve and n is the refractive index of the solvent, with the subscripts “s” and “r” representing sample and reference respectively [48]. Doped thin film were obtained by spin-coating a DCM solution (1 mL) of a mixture of the sample (1 mg) and the PMMA (19 mg) matrix onto a quartz glass. Differential scanning calorimetry (DSC) analyses were performed on a Perkin-Elmer Pyris Diamond DSC under nitrogen purge at a heat rate of 20 ^{o}C/min. Thermogravimetric analyses (TGA) were achieved with a Perkin-Elmer TGA-6 thermal analyzers under nitrogen at a heat rate of 40 ^{o}C/min. Cyclic voltammetry measurements were performed on a BAS CV-50W electrochemical analyzer adapted with a conventional three-electrode configuration consisting platinum working and auxiliary electrodes and a Ag/AgCl reference electrode. All measurements were effected in 0.1 M THF solution with tetrabutylammonium hexafluorophosphate as the supporting electrolyte and ferrocene as the internal standard. Molecular weights were determined by Gel Permeation Chromatography (GPC) using a HP 1050 series HPLC with THF as the eluent and a UV absorption detector (at 254 nm) calibrated against polystyrene MW standards.

Materials. All the commercially available chemicals and reagent grade solvents were used as received. Anhydrous THF was obtained from distillation over sodium benzophenone ketyl. Toluene used in polymerization was distilled fresh once from calcium hydride and AIBN was recrystallized from methanol before use.

Synthesis

10-Methylphenothiazine (1)

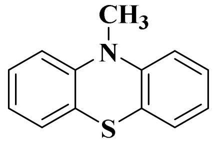

To a solution of phenothiazine (5 g, 25.1 mmol) in dry THF (30 ml) under stirring at room temperature blanketed with nitrogen, potassium *tert*-butoxide (4.22 g, 37.7 mmol) was added. The suspension was allowed to stir for 10 minutes, followed by dropwise addition of methyl iodide (2.35 ml, 37.7 mmol). After stirring for another 30 minutes, excess hexane (50 ml) was added and the whole mixture was filtered through a short plug of silica. The silica was then washed with DCM several times. The filtrate was concentrated and dried under vacuum to give the crude **1** as a purple solid (5.24 g, 98%) which was used directly for subsequent procedures. Mp 100.8-101.6 ^{o}C (lit. 101.7 ^{o}C -104.1 ^{o}C) [49].

3-Formyl-10-methylphenothiazine (2)

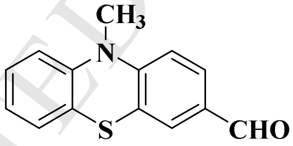

A mixture of **1** (6.74 g, 31.6 mmol), phosphorus oxychloride (16.1 ml, 173 mmol), dimethylformamide (11.5 ml, 149 mmol) in chlorobenzene (20 ml) was heated at 70 ^{o}C for 5 hours. After cooling, ice water was added and the mixture was neutralized by sat. $NaHCO_3$ (aq). The mixture was then allowed to stir for about another half an hour to ensure complete hydrolysis of the imine immediate which was then extracted by DCM (20 mL x 3). The combined organic phase was washed with sat. $NaHCO_3$ (aq) and then brine. The DCM solution was dried with anhydrous Mg_2SO_4 and concentrated in vacuo to give the crude which was purified by flash column chromatography using EA: Hexane: Triethylamine (1:5:2%) as eluent to offer **2** (6.28

g, 81.5%) as a yellow solid. mp 83.1-83.9 ^{o}C; δ_H (CDCl$_3$) 9.77 (s, 1 H), 7.63 (dd, *J* = 8.4 and 2.0 Hz, 1 H), 7.57 (d, *J* = 2.0 Hz, 1 H) , 7.19-7.14 (m, 1 H), 7.10 (dd, *J* = 7.6 and 1.6 Hz, 1 H), 6.96 (dt, *J* = 7.6 and 1.6 Hz, 1 H), 6.83 (d, *J* = 8.4 Hz, 1 H), 6.82 (dd, *J* = 8.0 and 0.8 Hz, 1 H), 3.39 (s, 3 H); δ_C (CDCl$_3$) 189.1, 150.0, 143.0, 130.1, 129.5, 126.9, 126.8, 126.3, 122.9, 122.6, 121.5, 113.8, 112.7, 34.8.

3-Cyano-10-methylphenothiazine (3)

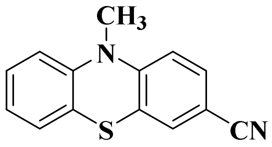

A mixture of **2** (2.91 g, 12.1 mmol) and hydroxylamine hydrochloride (2.52 g, 36.3 mmol) in NMP (30 ml) was heated to 120 ^{o}C overnight. After cooling, water was added and the mixture was extracted by DCM for several times. The combined organic phase was washed with water for three times and finally with brine. The DCM solution was dried by anhydrous Mg$_2$SO$_4$ and concentrated in vacuo to give the crude which was purified by flash column chromatography using EA: Hexane: Triethylamine (1:6:2%) as eluent to offer **3** (2.40 g, 83.6%) as a white solid. mp 122.0-122.8 ^{o}C; δ_H (CDCl$_3$) 7.40 (dd, *J* = 8.0 and 2.0 Hz, 1 H), 7.29 (d, *J* = 2.0 Hz, 1 H), 7.18 (dt, *J* = 7.4 and 1.2 Hz, 1 H), 7.09 (dd, *J* = 7.4 and 1.2 Hz, 1 H), 6.97 (dt, *J* = 7.4 and 1.2 Hz, 1 H), 6.82 (d, *J* = 8.0 Hz, 1 H), 6.75 (d, *J* = 8.0 Hz, 1 H), 3.36 (s, 3 H); δ_C (CDCl$_3$) 149.6, 144.1, 132.0, 130.0, 128.0, 127.4, 124.5, 123.7, 122.0, 118.9, 114.8, 114.0, 105.3, 35.6.

3-(2*H*-tetrazol-5-yl)-10-methylphenothiazine (4)

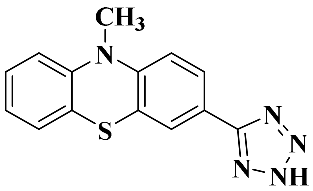

A mixture of **3** (760 mg, 3.19 mmol), sodium azide (621 mg, 9.55 mmol) and ammonium chloride (511 mg, 9.55 mmol) in DMF (20 ml) was heated at 115 ^{o}C for 2 days. After cooling, the reaction mixture was poured into water and acidified to pH 1 by conc. HCl (aq). The solid precipitated was filtered and air-dried overnight to offer **4** (780 mg, 86.9%) as a grey solid which was pure enough to be used directly in the next step. Mp: decomposed at 130 ^{o}C evidenced by gas formation (powder expanded from inside out and turned into foam.) δ_H (DMSO-*d*6) 7.88 (dd, *J* = 8.5 and 2.0 Hz, 1 H), 7.78 (d, *J* = 2.0 Hz, 1 H), 7.27-7.23 (m, 1 H), 7.20 (dd, *J* = 7.9 and 1.6 Hz, 1 H), 7.14 (d, *J* = 8.6 Hz, 1 H), 7.03-6.99 (m, 2 H), 3.38 (s, 3 H); δ_C (DMSO-*d*6) 148.1, 144.8, 128.6, 127.4, 127.3, 125.4, 123.6, 123.5, 121.6, 118.4, 115.6, 35.9.

*General Procedures for the preparation of Phenothiazine-Oxadiazole Push-Pull Fluorophores (**5-9**)*

3-[5-(4-Toluyl)-1,3,4-oxadiazol-2-yl]-10-methylphenothiazine (PO-Tol, 6)

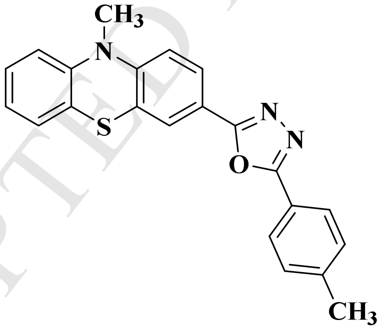

p-Toluyl chloride (0.18 ml, 1.36 mmol) was added dropwise to a solution of **4** (192 mg, 0.68 mmol) in dry pyridine (2 ml) and refluxed overnight. After cooling, 10% HCl (aq) (10 ml) was added to the mixture which was then extracted by DCM for several times. The combined organic was washed with sat. $NaHCO_3$ (aq) and then brine. The DCM solution was dried by anhydrous Mg_2SO_4 and concentrated in vacuo to give the crude which was purified by flash column chromatography using EA: Hexane: Triethylamine (1:4:2%) as eluent to offer **6** (142 mg, 48.9% from **3**) as a green solid. mp 143.4-144.2 ^{o}C; δ_H (CDCl$_3$) 7.98 (d, *J* = 8.0 Hz, 2 H), 7.91 (dd, *J* = 8.4 and 2.0 Hz, 1 H), 7.83 (d, *J* = 1.6 Hz, 1 H), 7.31 (d, *J* = 8.0 Hz, 2 H), 7.19-7.12 (m, 2 H), 6.96 (t, *J* = 7.6 Hz, 1 H), 6.86 (d, *J* = 8.4 Hz, 1 H), 6.83 (d, *J* = 8.0 Hz, 1 H), 3.40 (s, 3 H), 2.41 (s, 3 H); δ_C (CDCl$_3$) 164.4, 163.8, 148.6, 144.6, 142.2, 129.8, 127.8, 127.3, 126.8, 126.6, 125.3, 124.2, 123.3, 122.5, 121.2, 118.0, 114.5, 114.1, 35.6, 21.7; **Anal. Calcd. for $C_{22}H_{17}N_3OS$:** C, 71.14%; H, 4.61%; N, 11.31%. Found: C, 70.98%; H, 4.56%; N, 11.55%. HRMS (MALDI) calcd for $C_{22}H_{17}N_3OS$: 371.1092; found: 371.1088.

3-[5-Methyl-1,3,4-oxadiazol-2-yl]-10-methylphenothiazine (PO-Me, 5)

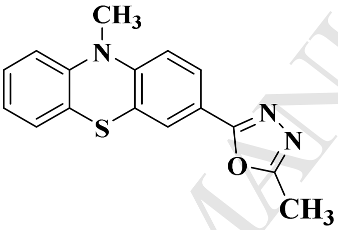

Yield: 42.0% from **3**. Yellow solid, mp 169.5-170.4 ^{o}C; δ_H (CDCl$_3$) 7.79 (d, *J* = 7.6 Hz, 1 H), 7.73 (s, 1 H), 7.19-7.11 (m, 2 H), 6.95 (t, *J* = 7.2 Hz, 1 H), 6.83 (d, *J* = 7.6 Hz, 1 H), 6.82 (d, *J* = 7.6 Hz, 1 H), 3.39 (s, 3 H), 2.57 (s, 3 H); δ_C (CDCl$_3$) 164.3, 163.2, 148.5, 146.7, 127.7, 127.3, 126.3, 125.2, 124.2, 123.2, 122.6, 118.0, 114.5, 114.1, 35.6, 11.7; **Anal. Calcd. for $C_{16}H_{13}N_3OS$:** C, 65.07%; H, 4.44%; N, 14.23%. Found: C, 64.83%; H, 4.56%; N, 14.30%. HRMS (MALDI) calcd for $C_{16}H_{13}N_3OS$: 295.0779; found: 295.0768.

3-[5-(2-Thiophenyl)-1,3,4-oxadiazol-2-yl]-10-methylphenothiazine (PO-Th, 7)

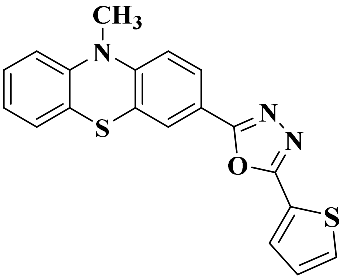

Yield: 66.7% from **3**. Green solid, mp 167.4-168.1 °C; δ_H (CDCl$_3$) 7.88 (dd, *J* = 8.4 and 2.0 Hz, 1 H), 7.80 (d, *J* = 2.0 Hz, 1 H), 7.79 (dd, *J* = 3.6 and 1.2 Hz, 1 H), 7.53 (dd, *J* = 5.2 and 1.2 Hz, 1 H), 7.20-7.15 (m, 2 H), 7.13 (dd, *J* = 7.6 and 1.6 Hz, 1 H), 6.96 (dt, *J* = 7.4 and 0.8 Hz, 1 H), 6.85 (d, *J* = 8.8 Hz, 1 H), 6.83 (dd, *J* = 8.0 and 0.8 Hz, 1 H), 3.39 (s, 3 H); δ_C (CDCl$_3$) 163.5, 160.5, 148.8, 144.6, 130.0, 129.6, 128.2, 127.8, 127.3, 126.6, 125.3, 124.2, 123.3, 122.5, 117.6, 114.6, 114.1, 35.6; **Anal. Calcd. for $C_{19}H_{13}N_3OS_2$:** C, 62.79%; H, 3.61%; N, 11.56%. Found: C, 62.88%; H, 3.56%; N, 11.31%. HRMS (MALDI) calcd for $C_{16}H_{13}N_3OS_2$: 363.0500; found: 363.0516.

3-[5-(9-Anthracenyl)-1,3,4-oxadiazol-2-yl]-10-methylphenothiazine (PO-An, 8)

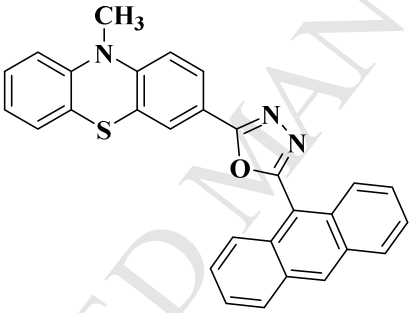

Yield: 46.1% from **3**. Yellow solid, mp 234.6-235.6 °C; δ_H (CDCl$_3$) 8.66 (s, 1 H), 8.08-7.94 (m, 5H), 7.87 (d, *J* = 2.0 Hz, 1 H), 7.54-7.51 (m, 4H), 7.17 (t, *J* = 8.0 Hz, 1 H), 7.11 (d, *J* = 7.2 Hz, 1 H), 6.95 (t, *J* = 7.6 Hz, 1 H), 6.88 (d, *J* = 8.4 Hz, 1 H), 6.83 (d, *J* = 8.0 Hz, 1 H), 3.42 (s, 3 H); δ_C (CDCl$_3$) 165.3, 162.6, 148.9, 144.6, 131.4, 131.0, 128.8, 127.7, 127.1, 126.8, 125.7, 125.5, 125.4, 125.1, 124.4, 123.3, 122.5, 117.9, 117.3, 114.6, 114.2, 35.6; **Anal. Calcd. for $C_{29}H_{19}N_3OS$:** C, 76.13%; H, 4.19%; N, 9.18%. Found: C, 76.28%; H, 4.11%; N, 9.30%. HRMS (MALDI) calcd for $C_{29}H_{19}N_3OS$: 457.1249; found: 457.1255.

3-[5-(2,3-Diphenylquinoxalin-6-yl)-1,3,4-oxadiazol-2-yl]-10-methylphenothiazine (PO-QX, 9)

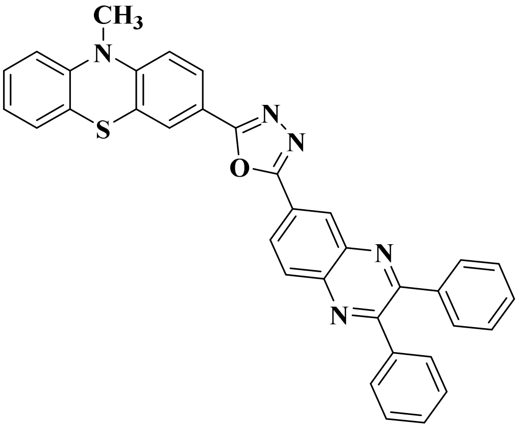

Yield: 55.9% from **3**. Orange solid, mp 244.6-245.4 °C; δ_H ($CDCl_3$) 8.87 (d, *J* = 1.6 Hz, 1 H), 8.54 (dd, *J* = 8.8 and 2.0 Hz, 1 H), 8.29 (d, *J* = 9.2 Hz, 1 H), 7.96 (dd, *J* = 8.4 and 2.0 Hz, 1 H), 7.90 (d, *J* = 2.0 Hz, 1 H), 7.54-7.52 (m, 4H), 7.38-7.33 (m, 6H), 7.20-7.14 (m, 2 H), 6.98 (dt, *J* = 7.4 and 0.8 Hz, 1 H), 6.91 (d, *J* = 8.8 Hz, 1 H), 6.85 (d, *J* = 8.0 Hz, 1 H), 3.43 (s, 3 H); δ_C ($CDCl_3$) 164.7, 163.5, 154.8, 154.7, 149.0, 144.5, 142.5, 140.9, 138.6, 138.5, 130.4, 129.9, 129.3, 128.4, 127.8, 127.6, 127.4, 126.7, 125.4, 125.1, 124.4, 123.4, 122.5, 117.6, 114.6, 114.2, 35.7; **Anal. Calcd. for $C_{35}H_{23}N_5OS$:** C, 74.85%; H, 4.13%; N, 12.47%. Found: C, 75.06%; H, 4.11%; N, 12.30%. HRMS (MALDI) calcd for $C_{35}H_{23}N_5OS$: 561.1623; found: 561.1638.

3-[5-(4-Toluyl)-1,3,4-oxadiazol-2-yl]-10-methylphenothiazine-*S,S*-dioxide (PO-Tol-SO$_2$, 10)

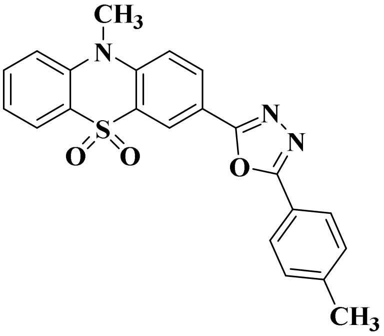

To **6** (250 mg, 0.67 mmol) and an excess of wet m-chloroperoxybenzoic acid (<77%, 1 g) was both dissolved in DCM (10 ml) was allowed to stir overnight. The reaction mixture was then washed with sat. $Na_2S_2O_3$ (aq) and then brine. The DCM solution was dried by anhydrous Mg_2SO_4 and concentrated in vacuo to give the crude which was purified by flash column chromatography using EA: Hexane: Triethylamine (1:1:2%) as eluent to offer **10** (267 mg, 99.3%) as a white solid. mp 251.4-252.4 ^{o}C; δ_H (DMSO) 8.58 (d, J = 2.0 Hz, 1 H), 8.42 (dd, J = 8.8 and 2.0 Hz, 1 H), 8.07 (dd, J = 8.0 and 2.4 Hz, 3 H), 7.85-7.81 (m, 2 H), 7.70 (d, J = 8.4 Hz, 1 H), 7.47-7.43 (m, 3 H), 3.82 (s, 3 H), 2.41 (s, 3 H); δ_C (DMSO) 164.2, 162.6, 143.4, 142.2, 141.0, 134.0, 131.1, 129.9, 126.7, 123.6, 123.5, 122.9, 122.5, 120.8, 120.5, 118.1, 117.4, 116.7, 36.2, 21.1; **Anal. Calcd. for $C_{22}H_{17}N_3O_3S$:** C, 65.49%; H, 4.25%; N, 10.42%. Found: C, 65.59%; H, 4.14%; N, 10.36%. HRMS (MALDI) calcd for $C_{22}H_{18}N_3O_3S$: 404.1069; found: 404.0636.

3-[5-(4-Toluyl)-1,3,4-oxadiazol-2-yl]-7-formyl-10-methylphenothiazine (11)

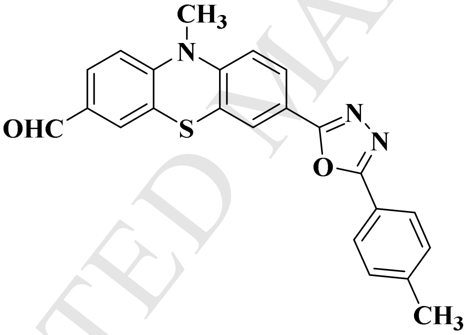

A mixture of **6** (1 g, 2.70 mmol), phosphorus oxychloride (2.74 ml, 29.5 mmol), dimethylformamide (2.0 ml, 25.4 mmol) in chlorobenzene (5ml) was heated to 100 ^{o}C for overnight. After cooling, ice water was added and the mixture was neutralized by sat. $NaHCO_3$ (aq). The mixture was allowed to stir for another half an hour to ensure complete hydrolysis of the imine immediate which was then extracted by DCM for several times. The combined organic phase was washed with sat. $NaHCO_3$ (aq) and then brine. The DCM solution was dried by anhydrous Mg_2SO_4 and concentrated in vacuo to give the crude which was purified by flash column chromatography using EA: Hexane: Triethylamine (1:1:2%) as eluent to offer **11** (552 mg, 51.2%) as an orange solid. mp 225.5-226.3 ^{o}C; δ_{H} ($CDCl_3$) 7.97 (d, *J* = 8.4 Hz, 2 H), 7.91 (dd, *J* = 8.4 and 2.0 Hz, 1 H), 7.79 (d, *J* = 2.0 Hz, 1 H), 7.65 (dd, *J* = 8.4 and 2.0 Hz, 1 H), 7.58 (d, *J* = 1.6 Hz, 1 H), 7.30 (d, *J* = 8.0 Hz, 2 H), 6.89 (d, *J* = 8.4 Hz, 1 H), 6.87 (d, *J* = 8.4 Hz, 1 H), 3.45 (s, 3 H), 2.41 (s, 3 H); δ_{C} ($CDCl_3$) 189.0, 164.6, 163.4, 149.9, 146.8, 142.3, 131.8, 130.6, 129.8, 128.0, 126.8, 126.7, 125.3, 123.6, 123.3, 121.1, 119.3, 114.9, 114.3, 3.61, 21.7; HRMS (MALDI) calcd for $C_{23}H_{17}N_3O_2S$: 399.1041; found: 399.1026.

3-[5-(4-Toluyl)-1,3,4-oxadiazol-2-yl]-7-vinyl-10-methylphenothiazine (PO-Tol-vinyl, 12)

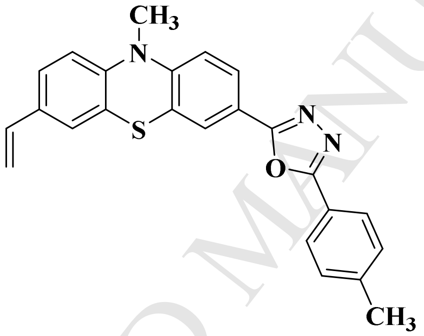

To a suspension of potassium *tert*-butoxide (281 mg, 2.51 mmol) and methyl triphenylphosphonium bromide (446 mg, 2.51 mmol) in dry THF (10 ml) was added dropwise into a dry THF (10ml) solution of **11** (500 mg, 1.25 mmol) at room temperature under stirring. The reaction mixture was allowed to stir for another half an hour. Hexane (20 ml) was added and the whole mixture was filtered through a short plug of silica, followed by washing with DCM for several times. The combined DCM solution was concentrated in vacuo to give the crude product which was purified by flash column chromatography with Hexane: EA: Triethylamine (4:1:2%) as eluent to offer **12** (472 mg, 95.2%) as a green solid. mp 179.3-180.1 ^{o}C; δ_{H} ($CDCl_3$) 7.99 (d, *J* = 8.4 Hz, 2 H), 7.90 (dd, *J* = 8.4 and 2.0 Hz, 1 H), 7.82 (d, *J* = 2.0 Hz, 1 H), 7.31 (d, *J* = 7.6 Hz, 2 H), 7.20-7.17 (m, 4 H), 6.58 (dd, *J* = 17.6 and 11.2 Hz, 1

H), 5.62 (d, J = 17.6 Hz, 1 H), 5.16 (d, J = 11.2 Hz, 1 H), 3.40 (s, 3 H), 2.42 (s, 3 H); δ_C ($CDCl_3$) 164.4, 163.8, 148.2, 144.0, 142.1, 135.2, 133.0, 129.7, 126.8, 126.5, 125.9, 125.3, 124.7, 123.8, 122.6, 121.1, 118.0, 114.4, 114.1, 112.9, 35.7, 21.7; HRMS (MALDI) calcd for $C_{24}H_{19}N_3OS$: 397.1249; found: 397.1241.

Poly(PO-Tol) (13):

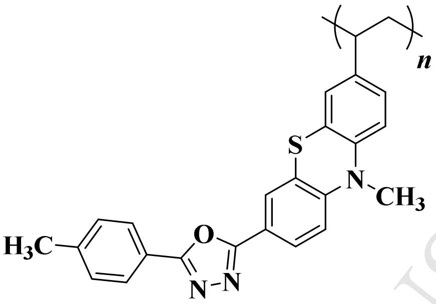

A solution of **12** (200 mg, 0.50 mmol) and catalytic AIBN (0.8 mg, 5 μmol) in toluene (1 mL) was degassed by freeze-pump-thaw techniques for 5 cycles, then heated at 80°C under nitrogen for overnight. After cooling, the solution was added dropwise to a stirring methanol and the precipitates thus formed were collected and further purified by Soxhlet extraction using methanol as the extraction solvent for 2 days. The resulting polymers were dried until constant weight (124.8 mg, 62.4%) as a light-green powder. δ_H ($CDCl_3$) 8.1-7.8 (br), 7.4-7.1 (br), 7.0-6.8 (br), 2.2-1.9 (br), 1.5-1.2 (br). M_n: 32,000 Da. PDI: 1.7. **Anal. Calcd. for $C_{24}H_{21}N_3OS$:** C, 72.15%; H, 5.30%; N, 10.52%. Found: C, 72.31%; H, 5.23%; N, 10.40%.

Acknowledgement

We are grateful to receive financial support for this work from the Hong Kong Research Grants Council (HKBU 2105/06E).

References

1. Uoyama H, Goushi K, Shizu K, Nomura H, Adachi C. Highly efficient organic light-emitting diodes from delayed fluorescence. Nature 2012;492:234-8.
2. Zhang Q, Li B, Huang S, Nomura H, Tanaka H, Adachi C. Efficient blue organic light-emitting diodes employing thermally activated delayed

fluorescence. Nat Photon 2014;8:326-32.

3. Kaji H, Suzuki H, Fukushima T, Shizu K, Suzuki K, Kubo S, Komino T, Oiwa H, Suzuki F, Wakamiya A, Murata Y, Adachi C. Purely organic electroluminescent material realizing 100% conversion from electricity to light. Nat Comm 2015;6:8476.
4. Wong MY, Hedley GJ, Xie G, Kölln LS, Samuel IDW, Pertegás A, Bolink HJ, Zysman-Colman E. Light-Emitting Electrochemical Cells and Solution-Processed Organic Light-Emitting Diodes Using Small Molecule Organic Thermally Activated Delayed Fluorescence Emitters. Chem Mater 2015;27:6535-42.
5. Qiu X, Xue S, Wu Y, Chen M, Sun Q, Yang W. Improving the electroluminescence performance of donor–acceptor molecules by fine-tuning the torsion angle and distance between donor and acceptor moieties. J Mater Chem C 2016:4:5988-95.
6. Wong MY, Zysman-Colman E. Purely Organic Thermally Activated Delayed Fluorescence Materials for Organic Light-Emitting Diodes. Adv Mater 2017:29:1605444.
7. Iqbal Z, Wu WQ, Huang ZS, Wang L, Kuang DB, Meier H, Cao D. Trilateral p-conjugation extensions of phenothiazine-based dyes enhance the photovoltaic performance of the dye-sensitized solar cells. Dyes Pigments 2016:124:63-71.
8. Huang ZS, Meier H, Cao D. Phenothiazine-based dyes for efficient dye-sensitized solar cells. J Mater Chem C 2016:4:2404-26.
9. He X, Cao B, Hauger TC, Kang M, Gusarov S, Luber EJ, Buriak JM. Donor−Acceptor Small Molecules for Organic Photovoltaics: Single-Atom Substitution (Se or S). ACS Appl Mater Interfaces 2015;7:8188-99.
10. Li Z, Zhu Z, Chueh CC, Jo SB, Luo J, Jang SH, Jen AKY. Rational Design of Dipolar Chromophore as an Efficient Dopant-Free Hole-Transporting Material for Perovskite Solar Cells. J Am Chem Soc 2016;138:11833-11839.
11. Kularatne RS, Magurudeniya HD, Sista P, Biewer MC, Stefan MC. Donor-Acceptor Semiconducting Polymers for Organic Solar Cells. J Polym Sci A Polym Chem 2013;51:743-68.
12. Ellinger S, Graham KR, Shi P, Farley RT, Steckler TT, Brookins RN, Taranekar P, Mei J, Padilha LA, Ensley TR, Hu H, Webster S, Hagan DJ, Stryland EWV, Schanze KS, Reynolds JR, Donor-Acceptor-Donor-based π-Conjugated Oligomers for Nonlinear Optics and Near-IR Emission. Chem Mater 2011;23:3805-17.
13. Chan CKM, Tao CH, Tam HL, Zhu N, Yam VWW, Cheah KW. Synthesis, Characterization, Luminescence, and Non-linear Optical Properties of Oxadiazole- and Truxene-Containing Platinum(II) Alkynyl Complexes with Donor-Acceptor Functionalities. Inorg Chem 2009;48:2855-2864.
14. Konidena RK, Thomas KRJ, Kumar S, Wang YC, Li CJ, Jou CJ. Phenothiazine Decorated Carbazoles: Effect of Substitution Pattern on the Optical and Electroluminescent Characteristics. J Org Chem 2015;80:5812-23.
15. Wan Z, Jia C, Duan Y, Zhou L, Lin Y, Shi Y. Phenothiazine–triphenylamine based organic dyes containing various conjugated linkers for efficient dye-sensitized solar cells. J Mater Chem 2012;22:25140-7.
16. Rodrigues T, Santos CGD, Riposati A, Barbosa LRS, Mascio PD, Itri R, Baptista MCS, Nascimento OR, Nantes IL. Photochemically Generated Stable Cation Radical of Phenothiazine Aggregates in Mildly Acid Buffered Solutions. J Phys Chem B 2006;110:12257−65.

17. Oka H. Synthesis and through-bond spin interaction of stable 1,3-phenylene linked poly(phenothiazine cation radical). J Mater Chem 2008;18:1927–34.
18. Lee J, Lee JI, Park MJ, Jung YK, Cho NS, Cho HJ, Hwang DH, Lee SK, Park JH, Hong J, Chu HY, Shim HK. Phenothiazine-*S,S*-dioxide- and Fluorene-Based Light-Emitting Polymers: Introduction of e$^-$-Deficient *S,S*-Dioxide into e$^-$-Rich Phenothiazine. J Polym Sci Part A Polym Chem 2007;45:1236-46.
19. Yao L, Sun S, Xue S, Zhang S, Wu X, Zhang H, Pan Y, Gu C, Li F, Ma Y. Aromatic S‑Heterocycle and Fluorene Derivatives as Solution-Processed Blue Fluorescent Emitters: Structure-Property Relationships for Different Sulfur Oxidation States. J Phys Chem C 2013;117:14189−96.
20. Liu Z, Shi E, Wan Y, Li N, Chen D, Xu Q, Li H, Lu J, Zhanga K, Wang L. Effects of gradual oxidation of aromatic Sulphur-heterocycle derivatives on multilevel memory data storage performance. J Mater Chem C 2015;3:2033-9.
21. Zhang Z, Wu Z, Sun J, Yao B, Zhang G, Xue P, Lu R. Mechanofluorochromic properties of β-iminoenolate boron complexes tuned by the electronic effects of terminal phenothiazine and phenothiazine-*S,S*-dioxide. J Mater Chem C 2015;3:4921-32.
22. Zhu L, Gu C, He Y, Wang G. Study on a highly selective fluorescent chemosensor for Cu^{2+} and its direct sensing for proton based on 1,3,4-oxadiazole. JOL 2014;153:439-45.
23. Zhou JA, Tang XL, Cheng J, Ju ZH, Yang LZ, Liu WS, Chena CY, Bai DC. An 1,3,4-oxadiazole-based OFF-ON fluorescent chemosensor for Zn^{2+} in aqueous solution and imaging application in living cells. Dalton Trans 2012;41:10626-32.
24. Landis CA, Dhar BM, Lee T, Sarjeant A, Katz HE. Syntheses, Solid State Structures, and Electrical Properties of Oxadiazole-Based Oligomers with Perfluorinated Endgroups. J Phys Chem C 2008;112:7939-45.
25. Wang C, Jung GY, Batsanov AS, Bryce MR, Petty MC. New electron-transporting materials for light emitting diodes: 1,3,4-oxadiazole-pyridine and 1,3,4-oxadiazole-pyrimidine hybrids. J Mater Chem 2002;12:173-180.
26. Liu R, Xu X, Peng J, Yao C, Wang J, Li L. Solution-processed oxadiazole-based electron-transporting layer for white organic light-emitting diodes. RSC Adv 2015;5:36568-74.
27. Lee J, Shizu K, Tanaka H, Nomura H, YasudaT, Adachi C. Oxadiazole- and triazole-based highly-efficient thermally activated delayed fluorescence emitters for organic light-emitting diodes. J Mater Chem C 2013;1:4599-604.
28. Kulkarni AP, Tonzola CJ, Babel A, Jenekhe SA. Electron Transport Materials for Organic Light-Emitting Diodes. Chem Mater 2004;16:4556-73.
29. Park YS, Choi J, Kim D, Lee B, Suh H, Kim JH. Synthesis, Optical, and Electroluminescent Properties of Alternating Copolymer Based on Phenothiazine and Fluorene with Oxadiazole Pendant. Mol Cryst Liq Cryst 2011:550:294-303.
30. Pan YZ, Wang YG, Liu JH, Sun LC. 10-Ethyl-3-(5-methyl-1,3,4-oxa-diazol-2-yl)-10*H*-pheno-thia-zine. Acta Cryst. E 2012:68:o649.
31. Ahn GH, Je EG, Kim JA, Kim JG, Yoo JU, Lee CM. Phenothiazine derivative as organic electroluminescent material and its preparing method. South Korea, KR 2012 129 582 A.
32. Jenekhe SA, Lu L, Alam MM. New Conjugated Polymers with Donor-Acceptor Architectures: Synthesis and Photophysics of Carbazole-Quinoline and Phenothiazine-Quinoline Copolymers and Oligomers Exhibiting Large

Intramolecular Charge Transfer. Macromolecules 2001;34:7315-24.

33. Kulkarni AP, Kong X, Jenekhe SA. High-Performance Organic Light-Emitting Diodes Based on Intramolecular Charge-Transfer Emission from Donor-Acceptor Molecules: Significance of Electron- Donor Strength and Molecular Geometry. Adv. Funct. Mater. 2006, 16, 1057-66.
34. Hancock JM, Gifford AP, Zhu Y, Lou Y, Jenekhe, SA. *n*-Type Conjugated Oligoquinoline and Oligoquinoxaline with Triphenylamine Endgroups: Efficient Ambipolar Light Emitters for Device Applications. Chem Mater 2006;18:4924-32.
35. Ishimatsu R, Matsunami S, Shizu K, Adachi C, Nakano K, Imato T. Solvent Effect on Thermally Activated Delayed Fluorescence by 1,2,3,5-Tetrakis(carbazol-9-yl)-4,6-dicyanobenzene. J Phys Chem A 2013;117:5607-12.
36. Thomas KRJ, Lin JT, Tao YT, Chuen CH, Green and Yellow Electroluminescent Dipolar Carbazole Derivatives: Features and Benefits of Electron-Withdrawing Segments. Chem Mater 2002;14:3852-9.
37. Saha S, Samanta A. Influence of the Structure of the Amino Group and Polarity of the Medium on the Photophysical Behavior of 4-Amino-1,8-naphthalimide Derivatives. J Phys Chem A 2002;106:4763-71.
38. Jia WL, Feng XD, Bai DR, Lu ZH, Wang S, Vamvounis G. Mes_2B(*p*-4,4’-biphenyl-NPh(1-naphthyl)): A Multifunctional Molecule for Electroluminescent Devices. Chem Mater 2005;17:164-70.
39. Islam A, Cheng CC, Chi SH, Lee SJ, Hela PG, Chen IC, Cheng CH. Aminonaphthalic Anhydrides as Red-Emitting Materials: Electroluminescence, Crystal Structure, and Photophysical Properties. J Phys Chem B 2005;109:5509-17.
40. Smallwood IM. Handbook of Organic Solvent Properties, 1st ed.; Butterworth-Heinemann: Oxford, 2012.
41. Duan,L, Hou L, Lee TW, Qiao J, Zhang D, Dong G, Wang, L Qiu Y. Solution processable small molecules for organic light-emitting diodes. J Mater Chem 2010;20:6392-407.
42. O'Brien DF, Burrows PE, Forrest SR, Koene BE, Loy DE, Thompson ME. Hole transporting materials with high glass transition temperatures for use in organic light-emitting devices. Adv Mater 1998;10:1108-12.
43. Shen JY, Yang XL, Huang TH, Lin JT, Ke TH, Chen LY, Wu CC, Yeh MCP. Ambipolar conductive 2,7-carbazole derivatives for electroluminescent devices. Adv Funct Mater 2007;17:983-95.
44. Naito K, Miura A. Molecular design for nonpolymeric organic dye glasses with thermal stability: relations between thermodynamic parameters and amorphous properties. J Phys Chem 1993;97:6240-8.
45. Wang S, Oldham Jr. WJ, Hudack Jr. RA, Bazan GC. Synthesis, morphology, and optical properties of tetrahedral oligo(phenylenevinylene) materials. J Am Chem Soc 2000;122:5695-709.
46. Wang W, Lin T, Wang M, Liu TX, Ren L, Chen D, Huang S. Aggregation Emission Properties of Oligomers Based on Tetraphenylethylene. J. Phys. Chem. B 2010:114:5983-8.
47. Wong MY, La-Placa MG, Pertegas A, Bolink HJ, Zysman-Colman E. Deep-blue thermally activated delayed fluorescence (TADF) emitters for light-emitting electrochemical cells (LEECs). J. Mater. Chem. C 2017:5:1699-703.
48. Melhuish MH. Quantum efficiencies of fluorescence of organic substances: effects of solvent and concentration of the fluorescent solute. J Phys Chem

1961;65:229-35.

49. McNeil SK, Kelley SP, Beg C, Cook H, Rogers RD, Nikles DE. Cocrystals of 10-methylphenthiazine and 1,3-dinitrobenzene: implications for the optical sensing of TNT-based explosives. ACS Appl Mater Interfaces 2013;5:7647-53.

Phenothiazine-oxadiazole dyads as a versatile sky-blue to green emitting scaffold

Combination of excellent quantum efficiency and electrochemical reversibility

Facile additional functionalization for tailored applications